PHYSICAL REVIEW E **80**, 011201 (2009)

Dynamic thermodiffusion model for binary liquid mixtures

Morteza Eslamian and M. Ziad Saghir[*]
Department of Mechanical and Industrial Engineering, Ryerson University, Toronto, Ontario, Canada M5B 2K3

(Received 22 April 2009; revised manuscript received 1 June 2009; published 20 July 2009)

Following the nonequilibrium thermodynamics approach, we develop a dynamic model to emulate thermodiffusion process and propose expressions for estimating the thermal diffusion factor in binary nonassociating liquid mixtures. Here, we correlate the net heat of transport in thermodiffusion with parameters, such as the mixture temperature and pressure, the size and shape of the molecules, and mobility of the components, because the molecules have to become activated before they can move. Based on this interpretation, the net heat of transport of each component can be somehow related to the viscosity and the activation energy of viscous flow of the same component defined in Eyring's reaction-rate theory [S. Glasstone, K. J. Laidler, and H. Eyring, *The Theory of Rate Processes: The Kinetics of Chemical Reactions, Viscosity, Diffusion and Electrochemical Phenomena* (McGraw-Hill, New York, 1941)]. This modeling approach is different from that of Haase and Kempers, in which thermodiffusion is considered as a function of the thermostatic properties of the mixture such as enthalpy. In simulating thermodiffusion, by correlating the net heat of transport with the activation energy of viscous flow, effects of the above mentioned parameters are accounted for, to some extent of course. The model developed here along with Haase-Kempers and Drickamer-Firoozabadi models linked with the Peng-Robinson equation of sate are evaluated against the experimental data for several recent nonassociating binary mixtures at various temperatures, pressures, and concentrations. Although the model prediction is still not perfect, the model is simple and easy to use, physically justified, and predicts the experimental data very good and much better than the existing models.

DOI: 10.1103/PhysRevE.80.011201 PACS number(s): 66.10.cd

I. INTRODUCTION

Spatial temperature gradient within a mixture of two or more components may cause mass diffusion: a process called thermodiffusion or Soret effect. In a mixture with a uniform temperature or small spatial temperature gradient, thermodiffusion is negligible and mass diffusion occurs if a concentration gradient exists within the mixture. Thermodiffusion has applications in several important processes in nature and technology exemplified by its crucial role in planning for oil extraction from the hydrocarbon reservoirs, which are subjected to relatively large temperature gradients [1,2]. Thermodiffusion is also important in isotropic separation of liquids [3], in emerging applications such as particle and molecule manipulation by temperature gradient (thermophoresis) [4,5], etc. Probably, the most accurate way of obtaining the thermal diffusion coefficients is by conducting experiments. However, obtaining accurate experimental data is challenging and expensive and, in some cases, impractical. Molecular-dynamics simulation [5,6] may also provide qualitative and semiquantitative results but is doable only for simple molecules and is also considered as time consuming and expensive. As a result, the development of theoretical models to predict the thermal diffusion coefficients with minimum effort is important for the design and control of pertinent processes and systems. Most of the classical thermodiffusion models developed for liquid mixtures are based on the nonequilibrium thermodynamics approach such as Drickamer and co-workers models [7–9], Haase [10] and Kempers [11,12] models, Firoozabadi and co-workers model [13,14], and Guy model [15]. Other approaches have been employed as well, such as the hydrodynamic and Brownian motion theory [16–19], fluctuation theory [20], kinetics theory [6], and so on. In a recent publication [21], we reviewed the existing thermodiffusion models, where we evaluated the merits of each model and classified the models as those needing a matching parameter, usually to be supplied from the outside of thermodynamics, and models that are rather self-reliant or independent. From another perspective, the models may be considered as either dynamic or static [22]. The static models rely on the thermostatic properties of the mixture, such as partial molar enthalpies only and, therefore, are similar to the nonmatching parameter models; whereas the dynamic models are those that regard the thermodiffusion phenomenon as dependent on the dynamic characteristics of the mixture and mass flow, as well as the mixture properties. Although not exactly the same, the dynamic models are similar to the matching parameter models. The best example of the matching parameter models are Drickamer and co-workers [7–9] and Firoozabadi and co-workers [13,14] models provided that the matching parameter is considered variable and mixture and temperature/pressure dependent. In these models, assigning a constant value to the matching parameter turns them into a static model. Examples of the nonmatching parameter or static models are Haase [10] and Kempers [11,12] models.

The predictions of the available models may be very different from one another and from the experimental data and reliable models even for binary mixtures are still lacking. This is because the thermodiffusion phenomenon in nonideal liquid mixtures is not understood adequately. Therefore, one of our goals in this paper is to elucidate some physical aspects of thermodiffusion as a dynamic process. In particular, starting from the linear nonequilibrium thermodynamics, we

---

[*] Corresponding author. zsaghir@ryerson.ca

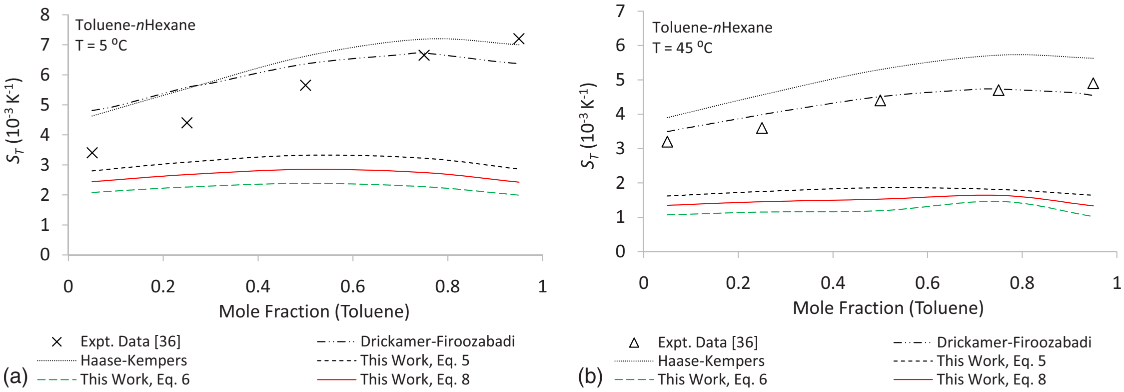

FIG. 1. (Color online) Experimental data and model prediction of the variation in the Soret coefficient S_T of toluene-*n*-hexane mixture versus mole fraction of toluene at (a) 5 °C and (b) 45 °C.

revisit and modify a model originally developed by Tichacek *et al.* [9] and propose several dynamic expressions for the calculation of the thermal diffusion factor in a binary mixture. The predictive power of the proposed expressions is examined against a large number of experimental data for binary nonassociating mixtures and also against the Haase-Kempers and Drickamer-Firoozabadi models linked with the Peng-Robinson equation of state (PR-EOS) [23].

II. MODEL DEVELOPMENT

Thermodiffusion in nonideal systems, such as liquid mixtures, is usually dealt with nonequilibrium thermodynamics. Starting from the Gouy-Stodola theorem in classic thermodynamics and assuming that the small elements of the system are in local equilibrium, an expression for the volumetric rate of entropy generation may be derived for a given system and used to define the conjugate forces and fluxes [24–26]. In linear nonequilibrium thermodynamics, for transport and rate processes, the heat and mass (molar) fluxes are assumed to be linear functions of forces, such as the gradients of temperature and chemical potentials. For an n-component mixture subjected to a body force, one can write the molar diffusion flux of component i with respect to component n and the mean molar velocity frame of reference, j_i (mole/m^{2}s), as a function of the appropriate thermodynamic forces for heat and mass transfer, i.e., $\nabla \ln T$ and $\nabla_T(\mu_k)$, and the net heat of transport of $n-1$ components as follows [24]:

$$j_i = -\sum_{k=1}^{n-1} L_{ik}[(Q_k^* - Q_n^*)\nabla \ln T + \nabla_T(\mu_k - \mu_n)], \qquad (1)$$

where L_{ik} are the phenomenological coefficients, Q_i^* (J/mole) is the net heat of transport of component i, which is the heat flow per mole of the diffusing component i, required to be absorbed during mass diffusion by the local region to keep the temperature constant. The net heat of transport in Eq. (1) is based on the diffusion flow j_i referred to the mean molar velocity. The flux of the component n, j_n is obtained differently and, based on the fact that in a mean molar frame of reference, the sum of all diffusive fluxes is zero. Note that depending on the choice of the reference component, the flux of component i would be written in $n-1$ different form. For a binary system, however, there will be only one independent flux and there is only one choice for the reference component.

Equation (1) may be used for any multicomponent system. For a binary nonhomogeneous, nonisothermal system, experimentalists usually use the following form of the diffu-

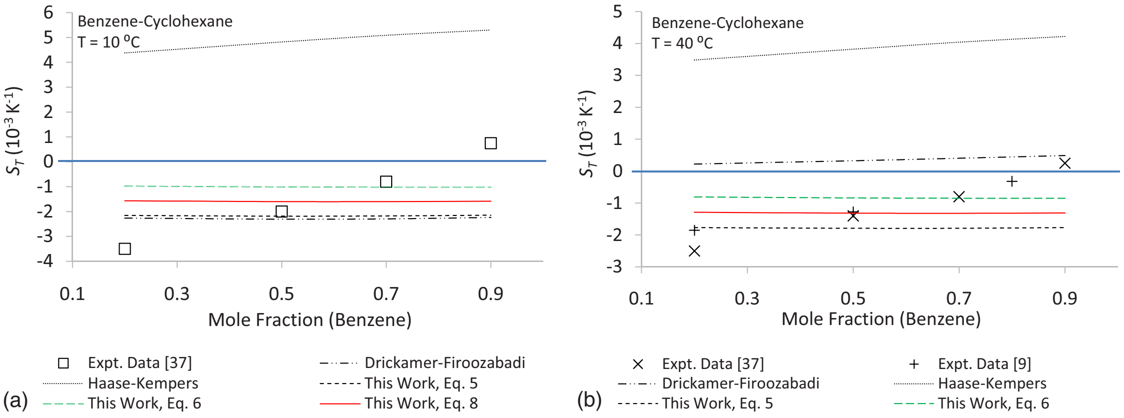

FIG. 2. (Color online) Experimental data and model prediction of the variation in the Soret coefficient S_T of benzene-cyclohexane mixture versus mole fraction of benzene at (a) 10 °C and (b) 40 °C.

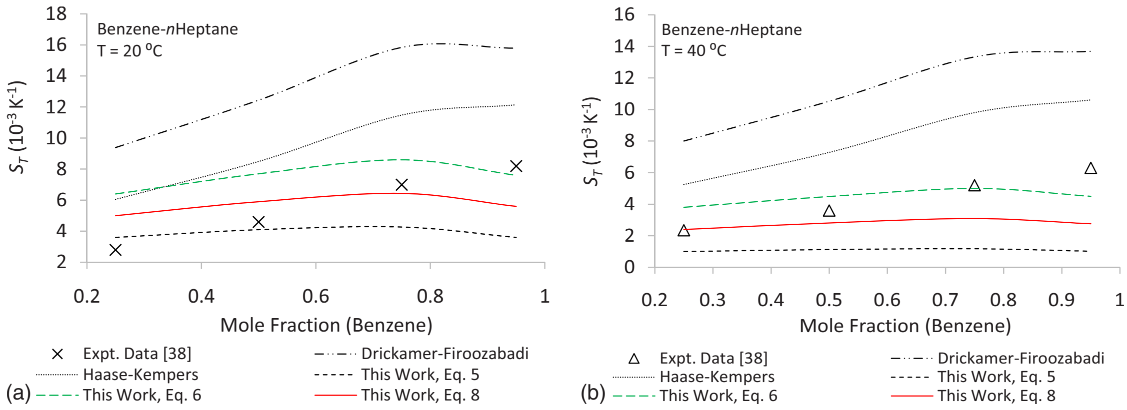

FIG. 3. (Color online) Experimental data and model prediction of the variation in the Soret coefficient S_T of benzene-*n*-heptane mixture versus mole fraction of benzene at (a) 20 °C and (b) 40 °C.

sive molar flux equation incorporating the thermal diffusion parameters:

$$j_1 = -cD_M\left[\nabla x_1 + \frac{\alpha x_1 x_2}{T}\nabla T\right] = -c[D_M \nabla x_1 + x_1 x_2 D_T \nabla T], \tag{2}$$

where c is the molar density (mole/m^3), x_1 and x_2 are the mole fractions of components 1 and 2, D_M is the Fickian or molecular mass diffusion coefficient (m^2/s), α is the thermal diffusion factor (nondimensional), D_T is the thermal diffusion coefficient (m^2/s K), and ∇T and ∇x are spatial temperature and concentration gradients. Note that following the Gibbs-Duhem equation, the gradients of chemical potential or concentration, temperature, and pressure are interrelated; therefore, in a nonisothermal and nonhomogenous system that is specified here, the pressure cannot be constant and there will be mass diffusion due to pressure gradient as well. This indicates that in Eq. (2), we have neglected the mass diffusion due to a pressure gradient. This may be justified because in typical applications, pressure diffusion compared to other effects is negligible. The complete form of the mass flux due to all forces is given by Firoozabadi and co-workers in Refs. [13,14].

In a binary system, thermal diffusion factor and coefficient are related to one another and to the Soret coefficient S_T through the following equation:

$$\alpha = TS_T = T\frac{D_T}{D_M}. \tag{3}$$

At the presence of a spatial temperature gradient ∇T, at steady-state mass transfer condition, the molar flux j_1 (and also j_2) vanishes. This condition combined with Eqs. (1) and (2) and the Gibbs-Duhem relation at constant pressure and temperature ($\Sigma x_i d\mu_i = 0$) results in the following approximate equation for the thermal diffusion factor in a binary system:

$$\alpha = \frac{Q_1^* - Q_2^*}{x_1(\partial \mu_1/\partial x_1)}. \tag{4}$$

Based on the chosen convention for the sign of α and D_T in Eq. (2), in a binary mixture if α (of component 1) obtained from Eq. (4) is positive, component 1 is enriched on the cold side.

Modeling of the net heat of transport has been the source of a great deal of confusion and discrepancies. Still a clear simulation for this quantity is lacking. The magnitude of the net heat of transport in thermodiffusion is a function of several local and global parameters, such as the mixture tem-

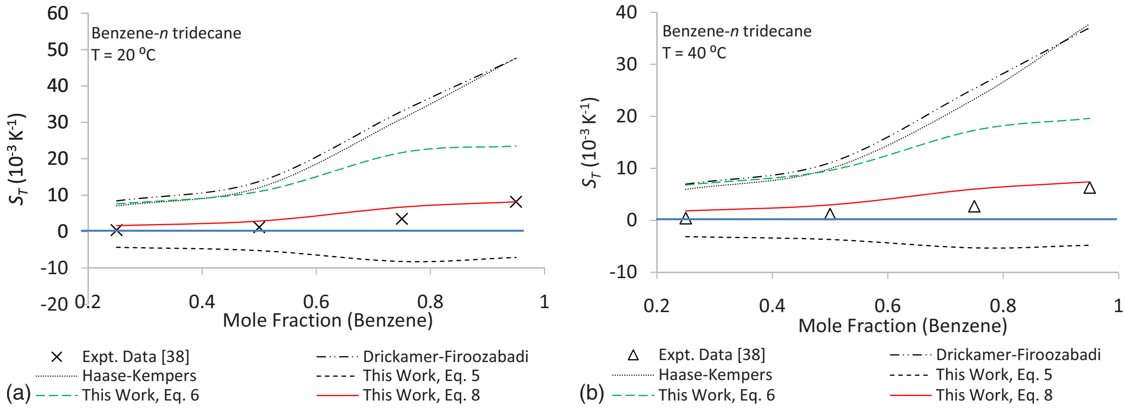

FIG. 4. (Color online) Experimental data and model prediction of the variation in the Soret coefficient S_T of benzene-*n*-tridecane mixture versus mole fraction of benzene at (a) 20 °C and (b) 40 °C.

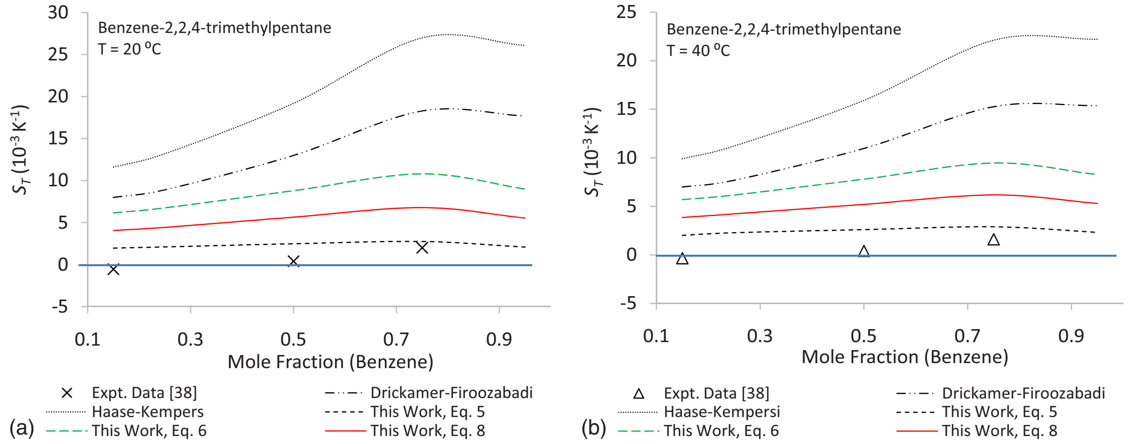

FIG. 5. (Color online) Experimental data and model prediction of the variation in the Soret coefficient S_T of benzene-2,2,4-trimethylpentane mixture versus the mole fraction of benzene at (a) 20 °C and (b) 40 °C.

perature and pressure, the size, density and shape of the molecules, and mobility or viscosity of the components. Static models, such as those of Haase [10] and Kempers [11,12], neglect the dependence of the heat of transport on the mobility of the components. Dynamic models of Dougherty and Drickamer [7,8] and Firoozabadi and co-workers [13,14] consider these effects but not adequately. Assigning a constant value to the matching parameter removes the dynamicity of the model.

Here, inspired from the work of Tichacek *et al.* [9], we correlate the net heat of transport with the activation energy of viscous flow. First, we may assume that the net heat of transport of each component equals the activation energy of viscous flow of that component in pure form, at the given mixture pressure and temperature (E^{vis}). Therefore, Eq. (4) may be written as follows:

$$\alpha = \frac{E_1^{vis} - E_2^{vis}}{x_1(\partial\mu_1/\partial x_1)}. \tag{5}$$

The molecular features that influence the thermodiffusion, such as the molecular size, shape, density, and moments of inertia [27,28]—to some extent—directly affect the viscosity data and, as a result, the activation energy of viscous flow, which is obtained directly from the viscosity data [29]. Here we are obtaining the activation energy of viscous flow of a liquid species in its pure state. In fact, to our knowledge, there is no theory that would define the activation energy of a component in a mixture. Besides, correlating and simulating the thermodiffusion phenomenon with viscous flow are an approximation, but it is a legitimate approach supported by physical evidence. As pointed out by Tichacek *et al.* [9] and followed by Artola *et al.* [6], a better agreement may be obtained if the net heat of transport is approximated by the activation energy of self-diffusion, which is of course not easy to determine.

Our calculations using the PR-EOS show that the denominator of Eq. (5), i.e., $x_1(\partial\mu_1/\partial x_1)=x_2(\partial\mu_2/\partial x_2)$, is rather insensitive to the species mole fractions x_1 and x_2. Also, since we obtain the activation energy of viscous flow of a component in the pure state, Eq. (5) predicts that varying the mixture compositions should have a minimum effect on the thermal diffusion factor. This is not supported by some of the experimental observations, as shown in the next section. Nevertheless, Eq. (5) should be able to provide an *average* value for the thermal diffusion factor in a mixture, when the relative molar fractions of the two components change.

In order to introduce the effects of mole fractions and molecular weights, a nonequilibrium thermodynamics approach similar to that of Dougherty and Drickamer [8] may be followed, where they modified Eq. (5) slightly to improve its accuracy by incorporating the effect of the species mole fractions. Again, here assuming that net heat of transport equals the activation energy of viscous flow of the same component in pure condition at the same pressure and temperature, the following equation is obtained:

$$\alpha = \frac{M_2E_1^{vis} - M_1E_2^{vis}}{(M_1x_1 + M_2x_2)x_1(\partial\mu_1/\partial x_1)}, \tag{6}$$

where M_1 and M_2 are the molecular weights of components 1 and 2. Similarly, in a molar volume frame of reference [9], Eq. (6) may be written as follows:

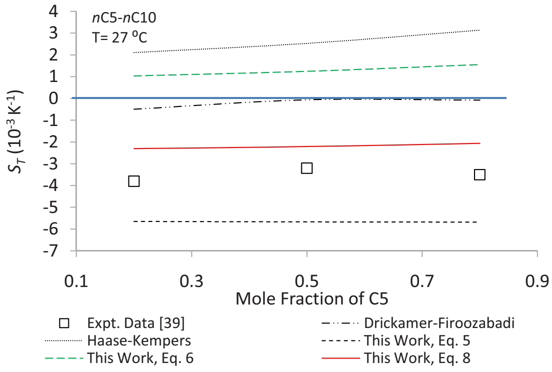

FIG. 6. (Color online) Experimental data and model prediction of the variation in the Soret coefficient S_T of nC$_5$-nC$_{10}$ mixture versus the mole fraction of pentane.

TABLE I. List of the experimental data used in this study.

Binary mixture	Temperature (°C)	Mole fraction of first component	Reference
toluene-*n*-hexane	5, 45	0.05,0.25,0.5,0.75,0.95	[36]
benzene-cyclohexane	10, 40	0.2,0.5,0.7,0.9	[37], [9]
benzene-*n*-heptane	20,40	0.25,0.5,0.75,0.95	[38]
benzene-*n*-tridecane	20, 40	0.25,0.5,0.75,0.95	[38]
benzene-2,2,4-trimethylpentane	20, 40	0.15,0.25,0.5,0.75,0.95	[38]
$n\mathrm{C}_i$-$n\mathrm{C}_{12}$, i: 5, 18	25	Mass fraction of $\mathrm{C}_i=0.5$	[2]
$n\mathrm{C}_5$-$n\mathrm{C}_{10}$	27	0.2,0.5,0.8	[39]
2-methylhexane-benzene	20,25,30,40	0.5	[38]
2,3-demethylpentane-benzene	20,30,40	0.5	[38]
$n\mathrm{C}_i$-benzene, i: 7–17	30	0.5	[38]
$n\mathrm{C}_{17}$-benzene	20,30,40	0.017	[38]
methane-*n*-butane[a]	121,46	0.4	[40]
$n\mathrm{C}_{10}$-$n\mathrm{C}_i$, i: 5–18	25	Mass fraction of $\mathrm{C}_{10}=0.25,0.75$	[41]
1-methylnaphtaline-$n\mathrm{C}_i$, i: 5–18	25	Mass fraction of 1-methylnaphtaline=0.25,0.75	[41]

[a] The pressure of methane-*n*-butane mixture ranges from 10 to 20 MPa, and for the rest of the mixtures is the atmospheric pressure.

$$\alpha=\frac{\bar{V}_2E_1^{vis}-\bar{V}_1E_2^{vis}}{(\bar{V}_1x_1+\bar{V}_2x_2)x_1(\partial\mu_1/\partial x_1)}, \tag{7}$$

where $\bar{V}_1$ and $\bar{V}_2$ are the partial molar volumes of components 1 and 2. Equation (7) is similar to that proposed by Tichacek *et al.* [9], where they modeled the net of transport as a *fraction* of the activation energy of viscous flow E_h^{vis}. They argued that the net heat of transport is that part of the activation energy of viscous flow that is transported with the moving molecules. However, since E_h^{vis} cannot be calculated systematically, Tichacek's model has not received much attention by others. Note that Eqs. (6) and (7) are similar to Haase and Kempers expressions, as well. The difference is that in Haase and Kempers expressions, the molar enthalpy has the same role as the activation energy of viscous flow in Eqs. (6) and (7). Since the molar enthalpy is a thermostatic property, Haase or Kempers model is a static model [21,22,30], whereas our expressions are dynamic because they relate thermodiffusion to a dynamic property, i.e., viscosity.

Careful consideration of the other thermodiffusion models particularly those of Artola *et al.* [6] and Debuschewitz and Köhler [31] revealed that these workers support this idea that the thermal diffusion factor in isotopic and other mixtures may be comprised of two or more terms, each of which responsible for different contributions, such as chemical interactions, molecular size and shape, etc. Therefore, similar to Artola's expression [6], here we propose the following equation for estimating the thermal diffusion factor, the weighted average of Eqs. (5) and (6):

$$\alpha=A\frac{M_2E_1^{vis}-M_1E_2^{vis}}{(M_1x_1+M_2x_2)x_1(\partial\mu_1/\partial x_1)}+B\frac{E_1^{vis}-E_2^{vis}}{x_1(\partial\mu_1/\partial x_1)}. \tag{8}$$

In Eq. (8), we have divided the thermal diffusion factor into two parts: the first term on the right-hand side has the molecular and to some extent the mole fraction effects, whereas the second term accounts for the difference in the activation energy of viscous flow and therefore incorporates some chemical effects. At this time, we cannot theoretically determine the values of A and B and, therefore, assume $A=B=\frac{1}{2}$, which corresponds to using the arithmetic mean of Eqs. (5) and (6). Evaluation of a broad range of hydrocarbon experimental data (next section) revealed that, in most cases, Eq. (8) with $A=B=\frac{1}{2}$ exhibits the best predictive power.

We have studied the predictive ability of the expressions developed here along with two other models, i.e., Kempers [11,12] and Shukla-Firoozabadi [13]. Kempers expressions were derived in a mass and volume frames of reference [11,12]. The expression written in a volume frame of reference highly overestimates the thermal diffusion factor and, therefore, for brevity it is not considered in the figures. Kempers expression written in a mass frame of reference is in fact the speculative expression of Haase [10] mathematically derived by Kempers [11,12]. Here we use a simplified version of this expression and call it the Haase-Kempers model. Note that in contrast to the other models, such as those of Drickamer [7–9], Firoozabadi [13], and Guy [15], Haase's expression for the overall thermal diffusion factor of a real mixture incorporates a "kinetic term," on account of the contribution of the ideal-gas state at the same temperature as the nonideal mixture under consideration. Later, Kempers followed the same approach and added this term in his expression in his second paper [12]. As pointed out by Kempers, in most cases the kinetic contribution is negligible. Kempers, instead of the direct calculation of this term, used it as a tuning parameter to calibrate his model for a better match with the experimental data. Here, neglecting the kinetic term and the properties of the initial states, the Haase-Kempers expression in a mass frame of reference is written as follows:

$$\alpha = \frac{M_1\bar{H}_2 - M_2\bar{H}_1}{(M_1x_1 + M_2x_2)x_1(\partial\mu_1/\partial x_1)}, \tag{9}$$

where $\bar{H}_1$ and $\bar{H}_2$ are the partial molar enthalpies of components 1 and 2, respectively. Note that Eq. (9) is very similar to Eq. (6).

The second model that is considered here is the binary model of Dougherty and Drickamer [7]; this model later was extended to the multicomponent mixtures and linked with the PR-EOS by Firoozabadi and his co-workers [13,14]. Here, we call this model, the Drickamer-Firoozabadi model,

$$\alpha = \frac{(\bar{U}_1 - \bar{U}^0_{1g})/\tau_1 - (\bar{U}_2 - \bar{U}^0_{2g})/\tau_2}{x_1(\partial\mu_1/\partial x_1)_{T,P}} + \frac{(\bar{V}_2 - \bar{V}_1)[x_1(\bar{U}_1 - \bar{U}^0_{1g})/\tau_1 + x_2(\bar{U}_1 - \bar{U}^0_{2g})/\tau_2]}{(x_1\bar{V}_1 + x_2\bar{V}_2)x_1(\partial\mu_1/\partial x_1)_{T,P}}, \tag{10}$$

where $\bar{U}_1$ and $\bar{U}_2$ are the partial molar internal energies of components 1 and 2, respectively. τ_i is a matching parameter interpreted as the ratio of the energy of vaporization of liquid component i to the activation energy of viscous flow of the same component (E^{vis}) defined by Eyring and co-workers [29]. However, both Drickamer and Firoozabadi assumed τ_i as a constant for all liquids with a value equal to 4.0. This assumption, in fact, turns this model from a dynamic model to a static model. Others, such as Saghir and his co-workers used variable τ_i as well [32–34], which is favored, because a variable matching parameter preserves the dynamicity of the model. E^{vis} and τ of each component may be determined by plotting the natural logarithm of the measured viscosity data multiplied by the molar volume ($\ln V\eta$) versus $1/RT$, where R is the universal gas constant and T is the mixture average temperature. When this plot is linear over a temperature range, the slope of the line is the activation energy of viscous flow over that range [21].

III. RESULTS AND DISCUSSION

The expressions proposed in this work and the Haase-Kempers and Drickamer-Firoozabadi models were linked with the PR-EOS; an in-house computer code was modified and used to calculate the mixture and components properties such as the partial molar enthalpy, internal energy, fugacity, etc. These properties are used to estimate the thermal diffusion factor or coefficient. The properties of the pure substances, such as the critical properties and viscosities, were extracted from the NIST database [35]. These properties are input data to the equation of state or needed to estimate the activation energy of viscous flow. Following the method 2 of Ref. [2], the matching parameters for each component required for the Drickamer-Firoozabadi model are assumed variable and were obtained using the viscosity data of that component in the pure state.

The models discussed here are at least applicable to all binary liquid mixtures. However, since the intermolecular forces between the associating molecules, such as water-alcohol mixtures are more complex than in the nonassociating mixtures (such as hydrocarbons), we limit our evaluation to the nonassociating mixtures. Due to the application of thermodiffusion in hydrocarbon reservoirs, most experimental investigations on nonassociating molecules have been performed on hydrocarbons. Table I lists the binary mixtures and their references used for model evaluation. Most of these data are very recent [36–39,41] and to our knowledge have not been compared to any theory before. Table II shows the activation energy of viscous flow of the liquids used in this study at various temperatures. The activation energies were obtained using the viscosity data [35] at the vicinity of each temperature.

The predictive power of Eq. (7), although in many cases better than those of Haase-Kempers and Drickamer-Firoozabadi models, was not better than Eqs. (5) and (8). Therefore, those results are not shown here.

TABLE II. Activation energy of viscous flow of the substances used in this study at various temperatures.

Substance	Temp. (K)	Activation energy (J/mole)
Benzene	298	9485.0
	313	9474.0
Cyclohexane	298	12112.0
	313	10897.0
Toluene	278	8364.0
	318	7783.0
2,2,4-trimethylpentane	293	8189.7
	313	7817.0
2-methylhexane	298	6818.0
	313	6886.7
2,3-demethylpentane	293	8184.0
	313	7973.8
1-methylnaphtalene	298	17786.0
n-pentane	298	5768.0
n-hexane	298	6593.0
n-heptane	298	7657.0
	313	8713.6
n-octane	298	8197.0
n-nonane	298	9310.0
n-decane	298	9990.0
n-undecane	298	11325.0
n-dodecane	298	11832.0
n-tridecane	298	12392.0
n-tetradecane	298	12695.0
n-pentadecane	298	13115.0
	303	13018.0
n-hexadecane	298	14983.0
n-heptadecane	293	14557.0
	298	13572.0
	303	13619.0
	313	13693.0
n-octadecane	298	16455.0

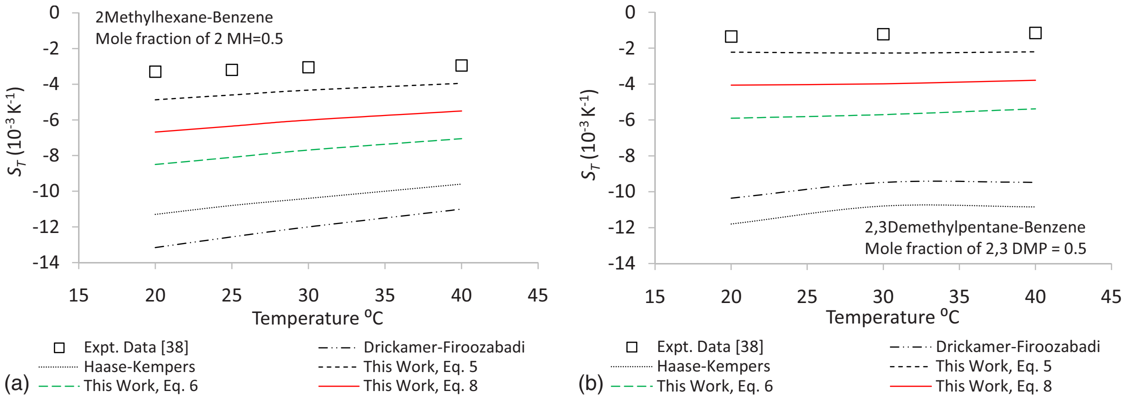

FIG. 7. (Color online) Experimental data and model prediction of the variation in the Soret coefficient S_T of (a) 2-methylhexane-benzene mixture and (b) 2,3-demethylpentane-benzene mixture with temperature.

A. Effect of temperature and concentration

As the first mixture, Fig. 1 shows the model and experimental data of the variation in the Soret coefficient for toluene-*n*-hexane mixture versus the mole fraction of toluene. In all figures, a positive value for the Soret coefficient S_T, thermal diffusion coefficient D_T, and thermal diffusion factor α indicates that the first component (A) in the binary mixture A-B is concentrated on the cold side. For this mixture, the Drickamer-Firoozabadi model is superior at both temperatures. Haase-Kempers and Eq. (7) of this work (not shown) can also satisfactorily predict the experimental data. Our other proposed expressions, i.e., Eqs. (5), (6), and (8) underestimate the Soret coefficient for this particular mixture. Now, if we consider the isotopic benzene-cyclohexane mixture (similar molecular weights), particularly at 40 °C, the Haase-Kempers and Drickamer-Firoozabadi models even cannot predict the sign of the Soret coefficient (see Fig. 2). Our proposed expressions and, particularly Eq. (8), can predict the sign and the average value of the Soret coefficient fairly good. However, for this isotopic mixture, none of the models can predict the significant change in the Soret coefficient with mole fractions. They rather predict an average value for the Soret coefficient over a range of various mole fractions. Haase-Kempers model, which is the most static model tested here, is the least favored model in predicting the experimental data. Figure 2 shows that at a very high concentration of benzene, the direction of mass transfer changes. Two sets of experimental data are shown in Fig. 2(b), one dates back to 50 years ago [9], and a recent one [38]; there is a very good agreement between these two sets of experimental data.

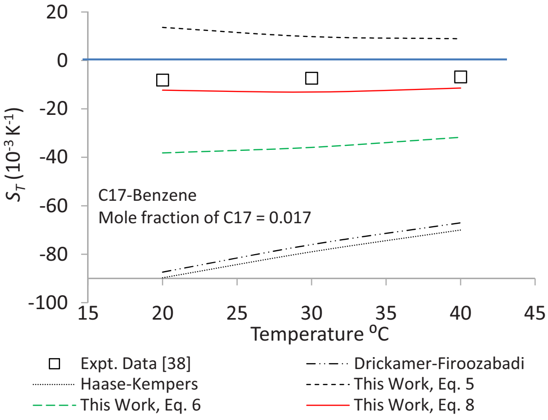

FIG. 8. (Color online) Experimental data and model prediction of the variation in the Soret coefficient S_T of heptadecane-benzene mixture versus temperature for given mole fractions.

To further investigate the predictive power of the models, we have shown the experimental data and model predictions for benzene-*n*-heptane mixture at 20 °C and 40 °C (Fig. 3). The Soret coefficient of benzene is *positive* and increases with the increase in benzene mole fraction. All models can predict this behavior to some extent. However, our proposed expressions also predict the magnitude of the Soret coefficient rather well. Equation (8) is in particular the best. Similar results are shown for benzene-*n*-tridecane mixture in Fig. 4. Note that even though benzene has a smaller molecular weight, the Soret coefficient of benzene in benzene-*n*-tridecane mixture is positive, which indicates that benzene migrates to the cold side. *n*-tridecane is forced to move in the opposite direction and goes to the hot side. Therefore, we may state that benzene is the dominant or more mobile component as it moves in the direction of heat transfer from hot to cold side, which may be considered as the more natural direction of mass transfer, as well. Normal alkanes, such as *n*-heptane and *n*-tridecane, are linear hydrocarbons, whereas benzene is an aromatic hydrocarbon with a cyclic nonlinear structure and a high density. Compared to the normal alkanes with comparable molecular weights, such as *n*-pentane and *n*-hexane, benzene is more viscous and, therefore, has larger activation energy of viscous flow. In thermodiffusion of binary mixtures, our model [Eq. (5)] predicts that the component that has the higher activation energy of viscous flow moves in the direction of heat flow, i.e., moves to the cold side. This may be a reason for the unusual behavior of benzene that despite its small molecular weight in benzene-*n*-heptane and even in benzene-*n*-tridecane mixtures, it migrates to the cold side. Therefore, here to clarify this general agreement in thermodiffusion literature "that the heavier component goes to the cold side," we may emphasize that the *denser* species or the more viscous species more likely migrate to the cold side. The Haase-Kempers and

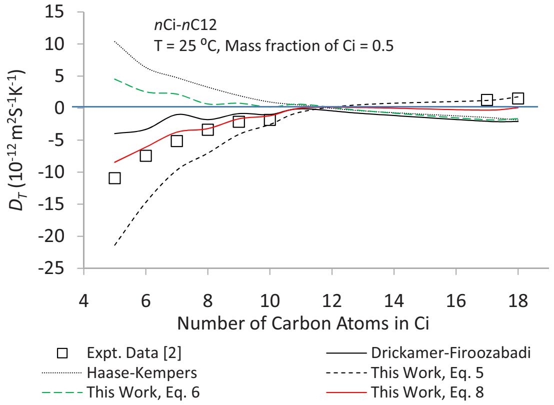

FIG. 9. (Color online) Experimental data and model prediction of the variation in the thermal diffusion coefficient D_T of $n\mathrm{C}_i$-$n\mathrm{C}_{12}$ mixture versus the number of carbon atoms in C_i.

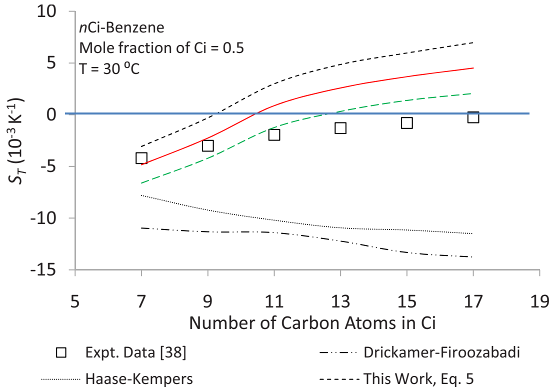

FIG. 10. (Color online) Experimental data and model prediction of the variation in the Soret coefficient S_T of $n\mathrm{C}_i$-benzene mixture versus the number of carbon atoms in C_i.

Firoozabadi-Drickamer models largely overestimate S_T. Our model predicts the experimental data much better and in fact Eq. (8) can successfully predict the data within a few percents error. In contrast to Fig. 1, where for the toluene-*n*-hexane mixture all models are rather insensitive to the mole fraction, for benzene-*n*-tridecane, all models show a much better sensitivity with respect to the change in mole fraction. An inspection of the mixtures studied so far shows that as the difference between the molecular weights of the two components increases, the models become more effective in a sense that they manage to show a change in the Soret coefficient when the mole fraction changes. In a similar case, Fig. 5 shows the model and experimental data for benzene-2,2,4-trimethylpentane mixture. The Soret coefficient of benzene in this mixture is rather small and, at low concentrations of benzene, it becomes negative. None of the models could predict this sign change. Nevertheless, our proposed expressions (5) and (8) show the best performance.

The model and experimental data for $n\mathrm{C}_5$-$n\mathrm{C}_{10}$ alkane mixture is shown in Fig. 6. Both molecules are linear and from the same family. *n*-pentane molecules have a smaller molecular weight, density, and activation energy and, as a result, are pushed to the hot side by the larger molecules of *n*-decane that naturally tend to move to the cold side; this is confirmed by the experimental data. The Drickamer-Firoozbadi model can hardly predict the sign, and the Haase-Kempers model fails to do so. The best prediction is made by our model [Eqs. (5) and (8)] similar to the previous case.

Two mixtures of heptane isomers and benzene, i.e., 2-methylhexane-benzene and 2,3-demethylpentane-benzene are studied in Fig. 7. For both cases, benzene migrates to the cold side. Haase-Kempers and Drickamer-Firoozabadi models highly overestimate the Soret coefficient. Our expressions, i.e., Eq. (5) and then Eq. (8), like most of the cases studied so far have a much better predictive ability. To interpret the experimental results of these binary mixtures based on our model, note that 2-methylhexane is less viscous than 2,3-demethylpentane and therefore has a smaller activation energy of viscous flow. As a result, our dynamic model predicts that 2-methylhexane should have a higher Soret coefficient (absolute value) than 2,3-demethylpentane both in benzene. This is indeed confirmed by the experimental data shown in Fig. 7.

The experimental and model data for *n*-heptadecane-benzene mixture at a low mole fraction of benzene (0.017) are displayed in Fig. 8. *n*-heptadecane has a long linear molecule with a much higher molecular weight than benzene, which is a cyclic low molecular weight but dense molecule. Due to the high density and rather high activation energy of viscous flow of benzene, it migrates to the cold side. Only our model and, in particular, Eq. (8) are able

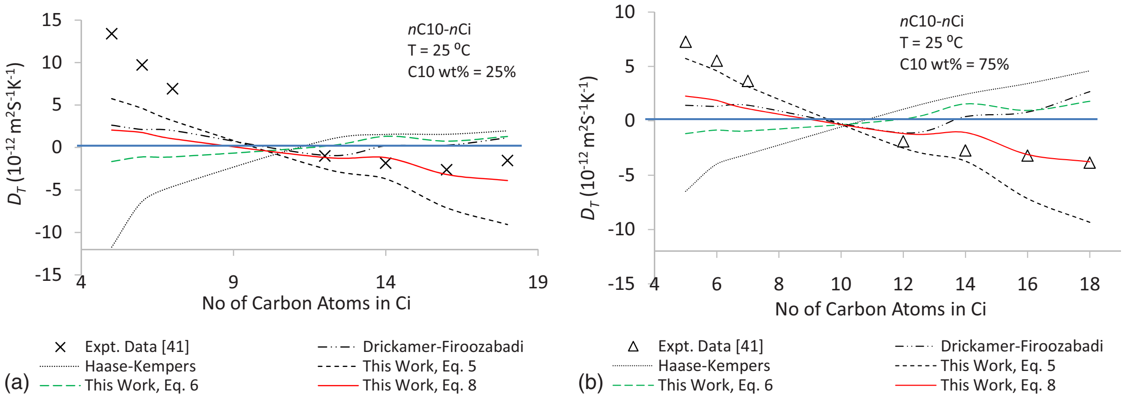

FIG. 11. (Color online) Experimental data and model prediction of the variation in the thermal diffusion coefficient D_T of $n\mathrm{C}_{10}$-$n\mathrm{C}_i$ mixture versus the number of carbon atoms in C_i. C_{10} wt % is (a) 25% and (b) 75%.

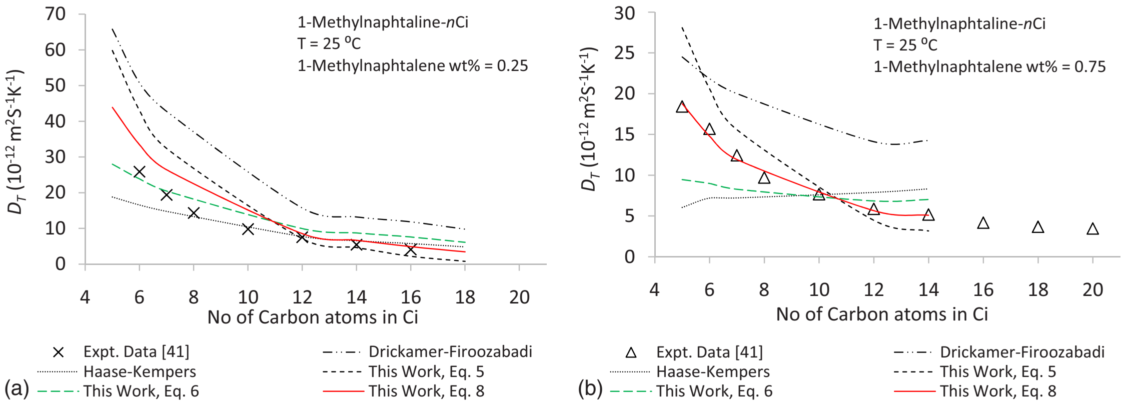

FIG. 12. (Color online) Experimental data and model prediction of the variation in the thermal diffusion coefficient D_T of 1-methylnaphtaline-$n\mathrm{C}_i$ mixture versus the number of carbon atoms in C_i. 1-methylnaphtalene wt % is (a) 0.25% and (b) 0.75%.

to predict the experimental data satisfactorily.

B. Effect of number of carbon atoms

In the foregoing experimental data, the variation in the Soret coefficient versus either temperature or mole fraction was studied. In the experimental data discussed in this section, the temperature and pressure, and either the mole or mass fraction of one of the species is constant, and the number of the carbon atoms of the second species in the mixture change. These cases can provide a measure of the overall capability of each model in predicting the experimental data. In Fig. 9, model and experimental data for thermal diffusion coefficient of binary $n\mathrm{C}_i$-$n\mathrm{C}_{12}$ mixtures are considered, where i varies from 5 (*n*-pentane) to 18 (*n*-octadecane), and mass fraction of C_i in all mixtures equals to 0.5. To convert the model thermal diffusion factors to thermal diffusion coefficients, the molecular diffusion coefficients were estimated using the Hayduk and Minhas correlation [42]. As expected and confirmed by the experimental observations, in those $n\mathrm{C}_i$-$n\mathrm{C}_{12}$ mixtures whose first component, i.e., C_i is lighter (has less density) than C_{12}, C_i is concentrated on the hot side; otherwise, it is enriched on the cold side. This is because all species in $n\mathrm{C}_\mathrm{i}$-$n\mathrm{C}_{12}$ are from the same family with similar molecular structures and, therefore, we can predict the sign of the Soret coefficient based on the molecular weight only, i.e., we can safely state that the larger molecule is concentrated on the cold side. Haase-Kempers model cannot even predict the sign of the thermal diffusion coefficient. Drickamer-Firoozabadi model is fairly good for $n\mathrm{C}_5$-$n\mathrm{C}_{12}$ to $n\mathrm{C}_{11}$-$n\mathrm{C}_{12}$ mixtures but fails to predict the mass transfer direction for $n\mathrm{C}_{17}$-$n\mathrm{C}_{12}$ and $n\mathrm{C}_{18}$-$n\mathrm{C}_{12}$ mixtures. As before, the best prediction is made by our two expressions (5) and (8). Equation (5) is more accurate for $n\mathrm{C}_{17}$-$n\mathrm{C}_{12}$ and $n\mathrm{C}_{18}$-$n\mathrm{C}_{12}$ mixtures, whereas Eq. (8) is better for $n\mathrm{C}_5$-$n\mathrm{C}_{12}$ to $n\mathrm{C}_{11}$-$n\mathrm{C}_{12}$ mixtures.

In a similar case, for $n\mathrm{C}_i$-benzene mixtures (Fig. 10), our expressions satisfactorily predict the trend of the variation in the Soret coefficient. The Haase-Kempers and Drickamer-Firoozabadi models predict an opposite trend for the Soret coefficient. Figures 11 and 12 show the variations in the thermal diffusion coefficient D_T of $n\mathrm{C}_{10}$-$n\mathrm{C}_i$ and 1-methylnaphtaline-$n\mathrm{C}_i$ mixtures, respectively. Only our expressions can satisfactorily predict the sign change; calculations made using Eq. (8) fairly match with the experimental data.

C. Effect of pressure

Analysis of the above-mentioned data showed that, in most cases, Eq. (8) is the superior expression for the estimation of the thermal diffusion factor for a large family of hydrocarbon binary mixtures. However, a prerequisite for using Eq. (8) is that at given mixture pressure and temperature, the pure components have to be in the liquid phase, so that their activation energies of viscous flow can be estimated. The same restriction applies to the Drickamer-Firoozabadi model, as well. On the other hand, the Haase-Kempers model is applicable to nonliquid mixtures as well. Having said that the Haase-Kempers model is the least-favored model in estimating the thermal diffusion factor of the hydrocarbon mixtures studied above, note that for the methane-*n*-butane mixture at high pressures, this model works very well (see Fig. 13). As argued before, the Haase-Kempers expression has been derived for the asymptotic condition, where the mixture is assumed to be at the thermostatic or equilibrium condition. Therefore, one may argue that for a mixture at very high pressures, mixture components are compressed and close to the ideal limit of being static and that is why the Haase-Kempers model can predict the experimental data in this condition rather well.

IV. CONCLUSIONS

In this study, inspired from the work of Tichacek *et al.* [9] and following the nonequilibrium thermodynamic principles, we introduced a dynamic model to simulate thermodiffusion process and proposed expressions for the estimation of thermal diffusion factor in binary liquid mixtures. In this model, the net heat of transport of each component defined in nonequilibrium thermodynamics was correlated with the activation energy of viscous flow to be obtained readily from the viscosity data. As the first approximation, the thermal diffusion factor was expressed by this expression $\alpha=(E_1^{vis}$

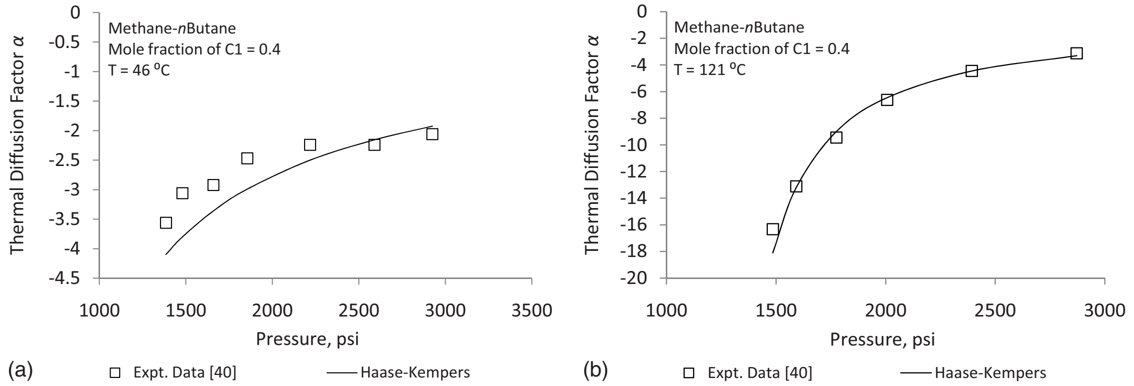

FIG. 13. Experimental data and model prediction of the variation in the thermal diffusion factor α of methane-*n*-butane mixture versus pressure. (a) $T=46\ ^\circ\mathrm{C}$ and (b) $T=121\ ^\circ\mathrm{C}$.

$-E_2^{vis})/x_1(\partial\mu_1/\partial x_1)$. We argued that since at least some of the properties of each component that affect the thermodiffusion phenomenon, such as the intermolecular chemical reactions and molecular shape, mass, and moments of inertia, also influence the component's viscosity and the activation energy of viscous flow, the proposed expression should be relatively successful in predicting the thermal diffusion factor, at least qualitatively. Furthermore, in order to highlight the effect of the molecular weights and mole fractions in the above-mentioned expression [Eq. (5)], we proposed a second expression, i.e., Eq. (8) for the estimation of the thermal diffusion factor, where an equal weight was assigned to the constant parameters, i.e., $A=B=\frac{1}{2}$. While the model is essentially applicable to both associating and nonassociating molecules, more than ten sets of experimental data for binary hydrocarbon mixtures (nonassociating molecules) proved the superiority of these expressions and, particularly, Eq. (8) over those of the well-known models of Haase [10], Kempers [11,12], Dougherty and Drickame [7], and Shukla and Firoozabadi [13], at least for the nonassociating molecules. All models were linked equally with the Peng-Robinson equation of state. Results of an ongoing research show that the modeling approach of this study is valid for the associating binary mixtures, such as water-alcohol, and for the multicomponent mixtures as well.

We also found that even though the Haase-Kempers model was the least accurate model for liquid mixtures studied under the atmospheric pressures and moderate temperatures, it was able to predict the experimental data of highly condensed gaseous mixture of methane-*n*-butane. Other models, such as Drickamer-Firoozabadi, and the model proposed here are limited to liquid mixtures only.

Finally, if one wishes to estimate the thermal diffusion factor in a binary mixture with minimum effort and without using an equation of state and just based on the viscosity data, the following expressions may be used:

$$\alpha = \frac{E_1^{vis} - E_2^{vis}}{RT}, \tag{5'}$$

$$\alpha = 0.5 \times \frac{M_2E_1^{vis} - M_1E_2^{vis}}{(M_1x_1 + M_2x_2)RT} + 0.5 \times \frac{E_1^{vis} - E_2^{vis}}{RT}. \tag{8'}$$

These equations are the simplified versions of Eqs. (5) and (8), where $x_1(\partial\mu_1/\partial x_1)$ has been approximated by RT.

ACKNOWLEDGMENTS

This research was supported by the Canadian Space Agency (CSA), the European Space Agency (ESA), and the National Science and Engineering Council Canada (NSERC). M.E. wishes to thank Ryerson University for the financial support.

---

[1] M. Khawaja, G. Jiang, S. Van-Vaerenbergh, and M. Z. Saghir, J. Non-Equilib. Thermodyn. **30**, 359 (2005).
[2] Y. Yan, P. Blanco, M. Z. Saghir, and M. M. Bou-Ali, J. Chem. Phys. **129**, 194507 (2008).
[3] S. Pan, G. Jiang, Y. Yan, M. Kawaji, and M. Z. Saghir, J. Non-Equilib. Thermodyn. **31**, 47 (2006).
[4] D. Vigolo, G. Brambilla, and R. Piazza, Phys. Rev. E **75**, 040401 (2007).
[5] G. Galliéro and F. Montel, Phys. Rev. E **78**, 041203 (2008).
[6] P.-A. Artola, B. Rousseau, and G. Galliero, J. Am. Chem. Soc. **130**, 10963 (2008).
[7] E. L. Dougherty, Jr. and H. G. Drickamer, J. Chem. Phys. **23**, 295 (1955).
[8] E. L. Dougherty, Jr. and H. G. Drickamer, J. Phys. Chem. **59**, 443 (1955).
[9] L. J. Tichacek, W. S. Kmak, and H. G. Drickamer, J. Phys. Chem. **60**, 660 (1956).
[10] R. Haase, *Thermodynamics of Irreversible Processes* (Addison-Wesley, Reading, MA, 1969).
[11] L. J. T. M. Kempers, J. Chem. Phys. **90**, 6541 (1989).
[12] L. J. T. M. Kempers, J. Chem. Phys. **115**, 6330 (2001).
[13] K. Shukla and A. Firoozabadi, Ind. Eng. Chem. Res. **37**, 3331 (1998).
[14] A. Firoozabadi, K. Ghorayeb, and K. Shukla, AIChE J. **46**,

892 (2000).
[15] A. G. Guy, Int. J. Thermophys. **7**, 563 (1986).
[16] J. Kreft and Y.-L. Chen, Phys. Rev. E **76**, 021912 (2007).
[17] S. N. Semenov and M. E. Schimpf, Phys. Rev. E **72**, 041202 (2005).
[18] H. Brenner, Phys. Rev. E **74**, 036306 (2006).
[19] K. I. Morozov, Phys. Rev. E **79**, 031204 (2009).
[20] A. A. Shapiro, Physica A **332**, 151 (2004).
[21] M. Eslamian and Z. Saghir, J. Non-Equilib. Thermodyn. **34**, 97 (2009).
[22] B. Faissat, K. Knudsen, E. H. Stenby, and F. Montel, Fluid Phase Equilib. **100**, 209 (1994).
[23] D. Y. Peng and D. B. Robinson, Ind. Eng. Chem. Fundam. **15**, 59 (1976).
[24] Y. Demirel and S. I. Sandler, Int. J. Heat Mass Transfer **44**, 2439 (2001).
[25] S. Kjelstrup and D. Bedeaux, *Non-Equilibrium Thermodynamics of Heterogeneous Systems* (World Scientific, Singapore, 2008).
[26] S. R. de Groot and P. Mazur, *Non-Equilibrium Thermodynamics* (Dover, New York, 1984).
[27] S. Wiegand, H. Ning, and R. Kita, J. Non-Equilib. Thermodyn. **32**, 193 (2007).
[28] G. Galliero, B. Duguay, J.-P. Caltagirone, and F. Montel, Fluid Phase Equilib. **208**, 171 (2003).
[29] S. Glasstone, K. J. Laidler, and H. Eyring, *The Theory of Rate Processes: The Kinetics of Chemical Reactions, Viscosity, Diffusion and Electrochemical Phenomena* (McGraw-Hill, New York, 1941).
[30] J. Farago, B. Rousseau, and P.-A. Artola, J. Chem. Phys. **125**, 164508 (2006).
[31] C. Debuschewitz and W. Köhler, Phys. Rev. Lett. **87**, 055901 (2001).
[32] S. Pan, M. Z. Saghir, M. Kawaji, G. Jiang, and Y. Yan, J. Chem. Phys. **126**, 014502 (2007).
[33] S. Pan, Y. Yan, T. J. Jaber, M. Kawaji, and M. Z. Saghir, J. Non-Equilib. Thermodyn. **32**, 241 (2007).
[34] M. Z. Saghir, G. Jiang, S. O. Derawi, E. H. Stenby, and M. Kawaji, Eur. Phys. J. E **15**, 241 (2004).
[35] Thermodynamic properties of hydrocarbon mixtures database, National Institute of Standards and Technology (NIST), version 3.2.
[36] K. J. Zhang, M. E. Briggs, R. W. Gammon, and J. V. Sengers, J. Chem. Phys. **104**, 6881 (1996).
[37] G. Wittko and W. Kohler, EPL **78**, 46007 (2007).
[38] P. Polyakov, J. Luettmer-Strathmann, and S. Wiegand, J. Phys. Chem. B **110**, 26215 (2006).
[39] A. Perronace, C. Leppla, F. Leroy, B. Rousseau, and S. Wiegand, J. Chem. Phys. **116**, 3718 (2002).
[40] W. M. Rutherford and J. G. Roof, J. Phys. Chem. **63**, 1506 (1959).
[41] A. Leahy-Dios, L. Zhuo, and A. Firoozabadi, J. Phys. Chem. B **112**, 6442 (2008).
[42] W. Hayduk and B. S. Minhas, Can. J. Chem. Eng. **60**, 295 (1982).